DISTRIBUTION OF GASES WITHIN APOLLO 15 SAMPLES; IMPLICATIONS FOR THE INCORPORATION OF GASES WITHIN SOLID BODIES OF THE SOLAR SYSTEM

George H. Megrue

Smithsonian Astrophysical Observatory, Cambridge, Massachusetts 02138

Submitted to the Journal of Geophysical Research, November 1972.

The distribution of helium, neon, and argon isotopes within Apollo 15 samples results primarily from fractionated solar-wind gases, accompanied by small quantities of cosmogenic gases. No unequivocal primordial lunar gases have been detected within various mineral, rock, or glass fragments. A vug from 15555 contains solar-wind gases that have abundance ratios similar to the Apollo 12 aluminum-foil experiments. A comparison of these Apollo 15 results with previous laser-probe mass spectrometric measurements from the gas-rich Kapoeta and Fayetteville meteorites, as well as with analyses of the Apollo 12 and 14 samples, indicates that the mechanism of solar-wind implantation followed by subsequent fractionation of the gases by impact brecciation and heating was primarily responsible for the incorporation of the original gas phase within solid bodies of the solar system.

INTRODUCTION

This study is directed toward measuring the relative concentration gradients of the helium, neon, and argon isotopes in selected Apollo 15 samples for the purpose of ascertaining (1) the spatial distribution of different gaseous constituents within the lunar solids and whether subsequent remobilization or homogenization of the gases occurred by thermal or shock events, (2) the possible source or sources of the various solids in the lunar regolith, and (3) the feasibility of measuring the temporal variations of the sources of the gases (in particular, with regard to the solar wind).

Previous laser-probe mass spectrometric measurements of individual mineral, glass, and clastic fragments, soil, and soil breccias from Apollo 12 [Megrue, 1971] and Apollo 14 [Megrue and Steinbrunn, 1972] samples demonstrate that variations in the relative abundances of the helium, neon, and argon isotopes occur down to and below the 10^{-4}-g level. Furthermore, profile analyses of individual glass and norite (KREEP) fragments show that relative elemental and isotopic abundances of the light rare gases are often highly variable between the surface and the interior of the fragments. Moreover, we have shown that ^{4}He and radiogenic ^{40}Ar from various glasses are correlated with the elemental distribution of potassium and that the solar-wind gases are not always limited to their expected range of a few microns but do occur within the interior of numerous glass and breccia samples. Consequently, the identification and relative abundances of the various types of gases within lunar samples can be used to classify and establish the origin or source of these materials. This is particularly important in determining whether lunar glasses and clastic rocks are the result of volcanic or impact processes.

In this analysis the following Apollo 15 samples were studied: glass-coated agglomerates (15245, 53) from station 6 along the Apennine Front; a green glass microbreccia (15426, 43) from station 7 at Spur Crater on the Apennine Front; four samples of a fine-grained breccia (15498, 37, 43, 54, 55) containing mare clasts and collected from station 4 at Dune Crater; and a vuggy gabbro (15555, 101) from station 9A at Hadley Rille [Swann et al., 1972].

EXPERIMENTAL RESULTS

Individual samples were analyzed by laser-probe mass spectrometry following the technique previously described [Megrue, 1970, 1971]. Generally, between 5 and 10 laser pulses were used to extract 10^{-5} g/pulse of material from selected portions of the lunar samples. The quantity of material extracted per laser pulse was calibrated by laser extraction of cosmogenic ^{3}He and ^{21}Ne from the previously analyzed Pena Blanca Springs meteorite (G. H. Megrue, unpublished, 1964). In using this calibration for lunar samples, we must assume that the lunar target material has similar physical properties (e.g., grain size, thermal conductivity, chemical composition) to those of the enstatite of Pena Blanca Springs.

Sensitivity of the mass-spectrometer system was determined by standard addition; i.e., known quantities of ^{3}He, ^{4}He, and atmospheric neon and argon were added to the mass spectrometer after analysis of each sample. During sample analysis, the sensitivity of the mass spectrometer varied by < 5%. Background corrections were applied to the laser-probe mass spectrometric measurements and are equivalent (in units of 10^{8} atoms) to $^{3}He = 24$, $^{4}He = 940$, $^{20}Ne = 62$, $^{21}Ne = 1$, $^{22}Ne = 3.2$, $^{36}Ar = 6.4$, $^{38}Ar = 2.0$, and $^{40}Ar = 640$.

GLASS-COATED AGGLOMERATES (15245, 53)

The concentration gradients of the helium, neon, and argon isotopes in this sample were determined by laser-probe mass spectrometric analysis of the glass coating, followed by profile analyses of the fine-grained matrix immediately below the glassy surface, then 5 mm below, and ultimately 8 to 10 mm below. The results (Table 1) demonstrate that the gases within the glass and fine-grained matrix are predominantly of solar-wind origin. The occurrence of solar-wind-implanted gases at a depth greater than a few microns within the fine-grained matrix indicates that this sample was formed from previously solar-irradiated lunar soil. Moreover, a comparison of the $^{4}He_{total}/^{36}Ar_{solar}$ and $(^{20}Ne/^{36}Ar)_{solar}$ (Figure 1) within the glass coating and fine-grained matrix indicates that the solar gases within the coating are fractionated relative to the gas within the matrix. This result leads us to infer that the glass coating of this sample was formed by melting of lunar soil that had been previously irradiated by the solar wind. Most likely, the melting of the soil was caused by meteorite impact and is not the result of volcanic processes.

Within a lithic fragment of 15245, 53, no solar gas was detected (Table 1); however, the $^{40}Ar/^{36}Ar = 12.7$ from this fragment is indicative of the presence of radiogenic ^{40}Ar.

GREEN ROCK (15426, 43)

This breccia sample of green glass spherules, collected from the rim of Spur Crater, was sieved into size fractions of < 100 mesh and > 60 mesh. Individual devitrified and nondevitrified spherules (green and black) were hand-picked from the > 60-mesh fraction and selectively analyzed by laser-probe mass spectrometry. The helium, neon, and argon isotopes within the individual spherules and the < 100-mesh size fraction (Table 2) consist of different proportions of cosmogenic and fractionated solar gases, as evidenced by the $^{20}Ne/^{22}Ne$, $^{21}Ne/^{22}Ne$, and $^{36}Ar/^{38}Ar$, which range from 6.4 to 13.2, 0.038 to 0.76, and 1.7 to 5.3, respectively.

Fractionation of the solar-type gases from the various spherule types is displayed graphically in Figure 1. The plotted values were derived by subtracting the cosmogenic component from the total elemental ratios. In particular, the spherules have $(^{20}Ne/^{36}Ar)_{solar}$ = 10 to 26 (which is much higher than we have observed in analyses of samples from the Apollo 12 and Apollo 14 missions) and $^{4}He_{total}/^{36}Ar_{solar}$ = 150 to 1050. No correction for radiogenic ^{4}He has been made to the total ^{4}He; consequently, the variation in the $^{4}He_{total}/^{36}Ar_{solar}$ may be the result either of different concentrations of radiogenic ^{4}He within the spherules or of a selective fractionation of the gases when the original solids of the lunar regolith were melted to produce the glass spherules.

BRECCIA 15498, 37, 43, 54, 55

Four samples of this breccia from Dune Crater were isotopically analyzed as part of a consortium investigation. Sample 37 (Figure 2), from an interior portion of the breccia, contains a fine glassy matrix, which is traversed by a fissure filling, probably of vesicular glass as described by Mason [1972] for other samples of 15498. Numerous light lithic fragments are also readily apparent. Samples 43, 54, and 55 are vesicular glasses from three different surface areas of the sample. The glass of sample 55 is underlain by a fine-grained matrix, which petrographically represents a completely different interior portion of the breccia than does sample 37 (Figure 3).

The results of the laser-probe mass spectrometric analyses of these samples (Table 3) show that the essential gaseous constituent of the sample is a highly fractionated solar-wind component. Cosmogenic gases are seen primarily within the light lithic fragment of sample 37 and fine-grained matrix of sample 55. The relative $^{4}He_{total}/^{36}Ar_{solar}$ versus $(^{20}Ne/^{36}Ar)_{solar}$ for the various samples of 15498, 37, 43, 54, 55 (Figure 1) are generally lower than the corresponding values measured in the other Apollo 15 samples. The fine matrix of 15498, 55 has a $^{4}He_{total}/^{36}Ar_{solar}$ nearly identical to that of the fine matrix of 15245, 53. This suggests, consequently, that these fine materials, which were collected from two different sites (Dune Crater and station 6 of the Apennine Front), were originally derived from the same source of lunar regolith. Moreover, the difference in the relative $^{4}He_{total}/^{36}Ar_{solar}$ and $(^{20}Ne/^{36}Ar)_{solar}$ from the fine-grained matrices of 15498, 55 and 15498, 37 indicates that these materials were originally derived from two completely different sources within the lunar regolith.

The relative $^{4}He_{total}/^{36}Ar_{solar}$ and $(^{20}Ne/^{36}Ar)_{solar}$ (Figure 1) from the three glass samples collected from the surface of breccia 15498 suggest that the glasses from samples 43 and 54, which contain highly fractionated solar gas, are derived from similar melted components of the lunar regolith. However, the relative $^{4}He_{total}/^{36}Ar_{solar}$ and $(^{20}Ne/^{36}Ar)_{solar}$ from the glass of sample 55 is completely different from the corresponding values of samples 43 and 54. This difference cannot be understood as resulting from relative differences of mass-fractionated solar gas; rather, it is produced by melting of the lunar regolith from two completely different sources. In fact, the $^{4}He_{total}/^{36}Ar_{solar}$ and $(^{20}Ne/^{36}Ar)_{solar}$ ratio from the glass of sample 55 suggests that this material may have been derived originally from a highly fractionated source identical with that of the fine glass spherules of 15426, 43.

VUGGY GABBRO (15555, 101)

The distribution of the helium, neon, and argon isotopes from within the mafic phase and a vug from the surface of the gabbro was determined by laser-probe mass spectrometry (Table 4) to be essentially derived from solar-wind implantation. Of particular interest is the fact that the $^4He/^{20}Ne$ and $^4He/^{36}Ar$ from the vug within the rock's surface are higher than the corresponding values from the mafic phase. The $^4He/^3He = 2400 \pm 200$ and $^4He/^{20}Ne = 630 \pm 60$ within the vug are consistent with the solar values reported by Geiss et al. [1970] from the Apollo 12 aluminum-foil solar-wind experiment and with the positive correlation between solar $^4He/^3He$ and $^4He/^{20}Ne$ that they deduced from other Apollo missions [Geiss et al., 1972].

Laser-probe mass spectrometric measurements of the gases within the feldspar constituents of the sample were not successful in determining the variation of solar, cosmogenic, or radiogenic gases.

DISCUSSION

Solar gases. From the preceding results, we conclude that various glass and breccia samples from Apollo 15 primarily contain fractionated solar gases in addition to undetermined quantities of radiogenic ^4He. A comparison of the $^4He_{total}/^{36}Ar_{solar}$ versus $(^{20}Ne/^{36}Ar)_{solar}$ from the Apollo 15 samples with previously determined laser-probe mass spectrometric analyses of the gas-rich Fayetteville and Kapoeta meteorites [Megrue, 1968] and of a typical sample from each of the Apollo 12 [Megrue, 1971] and Apollo 14 missions [Megrue and Steinbrunn, 1972] demonstrates that relative abundances of the solar gases within all these samples can be understood as resulting from various degrees of fractionated solar gas in addition to the presence of different quantities of radiogenic ^{4}He. In Figure 1 the dashed line was drawn to represent the trend of gas fractionation if we assume a simple diffusion model that varies as the square root of the relative masses. This line has been extrapolated from the lunar value of $^4He/^{20}Ne = 100$. In one direction, it is observed to intersect the solar $^4He/^{36}Ar$ and $^{20}Ne/^{36}Ar$ as measured in the Fayetteville meteorite, and in the other, the corresponding values as measured in the Apollo 15 materials. If this simple interpretation is correct, then points that lie significantly above the curve are suspected to contain radiogenic ^{4}He, as our analyses of Apollo 14 glasses [Megrue and Steinbrunn, 1972] have previously demonstrated. Samples that contain $(^{20}Ne/^{36}Ar)_{solar}$ lying to the right of the curve, as does lunar green glass 15426, 43, may result from the differences in the relative diffusivities of rare gases from different minerals or from another rare-gas component, such as indigenous lunar neon. Only future research can resolve these alternate explanations.

Since most of the solar gas within lunar samples appears to be highly fractionated and since the distribution of the gas within the interior of glass and breccia samples indicates that this gas was incorporated at a range greater than a few microns, then the mechanism responsible for the formation of these samples can be assumed to result from impact brecciation and redistribution of gases from previously solar-irradiated materials.

From the foregoing discussion of the presence of fractionated solar gases and of radiogenic ^{4}He within lunar samples, it might be concluded that a study of the temporal variations of the solar wind within lunar samples is doomed to a high degree of uncertainty, or failure. However, the relative abundances of the solar gases within a vug of 15555, 101 are entirely compatible with the result derived by the aluminum foil solar-wind experiments [Geiss et al., 1970] and indicate that vugs, which act as naturally occurring Faraday cages, may in fact be very efficient collectors of previous solar-wind irradiations. Future study of solar gases within vugs of lunar materials from different environments and ages could elucidate this possibility.

Cosmogenic gases. A plot of the $^{21}Ne/^{22}Ne$ versus $^{36}Ar/^{38}Ar$ from various Apollo 15 samples (Figure 4) displays an inverse correlation that is attributed to the addition of varying amounts of cosmogenic gas to the fractionated solar gases within the samples. Large variations in the cosmogenic ^{36}Ar and ^{38}Ar are primarily the result of variations in the calcium abundances. Of particular importance are the differences in the relative concentrations of the cosmogenic gases within the different types of spherules of 15426,43. The black spherules have the largest percentage of cosmogenic gas, whereas the green spherules contain the least and the devitrified spherules have an intermediate value. It is difficult to understand these differences in terms of chemical variations within the samples. Most likely, these variations reflect different cosmic-ray exposure ages because they come from different locations within a particular source (shielding effect) or because they are a mixture of materials from different sources.

Possible sources for Apollo 15 samples; implications for the lunar crust and early gas phase of solid bodies. It should be recalled that one of the primary objectives in the selection of the Apollo 15 site was to examine and collect samples brought up from lunar depths as great as 50 km by the Imbrium event and to compare them with the Apollo 14 rocks collected from the Fra Mauro formation, which is believed to represent the upper 5 km of the Imbrium structure. The results of our studies relate to this topic.

The welded 15498 breccia, which consists of interstitial glass and mare fragments and was collected from the south rim of Dune Crater, is thought to have been locally derived by brecciation and shock heating of regolith material when Dune Crater was formed by impact. This mechanism is consistent with the observed highly fractionated solar-gas abundances found within the glass coatings and matrix of this breccia. Furthermore, lunar soil appears to have been transported ~ 1.5 km by the impact event from the Dune Crater locality to station 6 on the Apennine Front, as evidenced by the similarity between the fractionated solar-gas abundances within the matrix and glass of 15498, 55 and the corresponding solar-gas abundances from the matrix and glass of 15426, 43.

The green glass 15426 from the Apennine Front represents a unique sample of the Apollo 15 collection. The unusual pyroxenite composition [Reid et al., 1972] of this material has resulted in the suggestion that this material was originally derived from 50-km depths by the Imbrium event. If this is true, then it is extremely important to note that this material contains fractionated abundances of solar-type gases that have high $^{20}Ne/^{36}Ar$ compared with other lunar materials (Figure 1). Consequently, the incorporation of the fractionated solar gas into the glass could have occurred only by a base surge process [Pai et al., 1972] instituted by heating of overlying solar-irradiated materials through impact melting followed by redistribution of the released gases within materials transported from great (50 km) depths.

The search for indigenous primordial lunar gases within vugs of 15555 has been unsuccessful and indicates that the concept of large quantities of primordial gases within the moon may be erroneous because of the previous insistence that carbonaceous chondritic material was the magic starting potion for the evolutionary development of planetary and lunar bodies. In fact, strong evidence from the analysis of gas-rich meteorites and lunar materials indicates that the early gas phase within planetary bodies was strongly reducing and was primarily the result of solar-implanted gases that were fractionated and redistributed with radiogenic gases [Megrue, 1972] by impact brecciation and accompanying thermal metamorphism.

Acknowledgments. This work was supported in part by NASA grant NGR 09-015-144.

REFERENCES

Geiss, J., P. Eberhardt, F. Bühler, J. Meister, and P. Signer, Apollo 11 and 12 solar wind composition experiments: Fluxes of He and Ne isotopes, J. Geophys. Res., 75, 5972, 1970.

Geiss, J., F. Bühler, H. Cerutti, and P. Eberhardt, Solar-wind composition experiment, Apollo 15 Preliminary Science Report, NASA SP-289, Sec. 15, 1, 1972.

Mason, B., Mineralogy and petrology of polymict breccia 15498, to be published in Apollo 15 Results, Lunar Science Institute, Houston, Texas, 1972.

Megrue, G. H., Distribution and origin of primordial helium, neon, and argon in the Fayetteville and Kapoeta meteorites, in Meteorite Research, edited by P. M. Millman, p. 922, D. Reidel Publ. Co., Dordrecht, Holland, 1968.

Megrue, G. H., Laser microprobe mass spectrometry with applications to meteorite research, in Recent Developments in Mass Spectroscopy, edited by K. Ogata and T. Hayakawa, p. 654, University of Tokyo Press, Tokyo, 1970.

Megrue, G. H., Distribution and origin of helium, neon, and argon isotopes in Apollo 12 samples measured by in situ analysis with a laser-probe mass spectrometer, J. Geophys. Res., 76, 4956, 1971.

Megrue, G. H., Spatial distribution of $^{40}Ar/^{39}Ar$ ages in lunar breccia 14301, submitted to J. Geophys. Res., 1972.

Megrue, G. H., and F. Steinbrunn, Classification and source of lunar soils; clastic rocks; and individual mineral, rock and glass fragments from Apollo 12 and 14 samples as determined by the concentration gradients of the helium, neon, and argon isotopes, Proc. of the 3rd Lunar Science Conf., MIT Press, Cambridge, Mass., in press, 1972.

Pai, S. I., T. Hsieh, and J. A. O'Keefe, Lunar ash flows: Isothermal approximation, J. Geophys. Res., 77, 3631, 1972.

Reid, A. M., J. Warner, W. Ridley, and R. Brown, Major element composition of glasses in three Apollo 15 soils, Meteoritics, 7, 395, 1972.

Swann, G. A., N. G. Bailey, R. M. Batson, V. I. Freeman, M. H. Hait, J. W. Head, H. E. Holt, K. A. Howard, J. B. Irwin, K. B. Larson, W. R. Muehlerger, V. S. Reed, J. J. Rennilson, G. G. Schaber, D. R. Scott, L. T. Silver, R. L. Sutton, G. E. Ulrich, H. G. Wilshire, and E. W. Wolfe, Preliminary geologic investigation of the Apollo 15 landing site, Apollo 15 Preliminary Science Report, NASA SP-289, Sec. 5, 1, 1972.

TABLE 1. Distribution of Helium, Neon, and Argon Isotopes in Glassy Soil Agglomerate 15245, 53

Location	^{4}He (10^{10} atoms/10^{-4} g)	$^{4}He/^{3}He$	$^{4}He/^{20}Ne$	$^{4}He/^{36}Ar$	$^{20}Ne/^{22}Ne$	$^{21}Ne/^{22}Ne$	$^{36}Ar/^{38}Ar$	$^{40}Ar/^{36}Ar$
Glass surface	2600	2100 ± 200	23 ± 2	83 ± 8	12.2 ± 0.3	0.040 ± 0.002	5.1 ± 0.1	1.4
Glass surface	1750	2100 ± 200	19 ± 2	46 ± 5	12.0 ± 0.3	0.038 ± 0.002	5.2 ± 0.1	2.8
Glass surface	800		19 ± 2	60 ± 6	10.3 ± 0.2	0.051 ± 0.002	4.0 ± 0.1	2.4
Fine matrix								
a) below glass	13500	1650 ± 165	29 ± 3	117 ± 10	13.1 ± 0.3	0.040 ± 0.002	5.2 ± 0.1	1.7
below glass	11300	1800 ± 180	30 ± 3	115 ± 10	12.8 ± 0.3	0.041 ± 0.002	5.2 ± 0.1	1.5
b) 5 mm below glass	11000	2600 ± 200	23 ± 2	113 ± 10	12.7 ± 0.3	0.038 ± 0.002	4.9 ± 0.1	1.7
c) 8 to 10 mm below glass	10600	2050 ± 200	33 ± 3	147 ± 10	12.5 ± 0.3	0.037 ± 0.002	5.4 ± 0.1	1.6
	15300	2500 ± 200	30 ± 3	155 ± 10	12.5 ± 0.3	0.035 ± 0.002	5.3 ± 0.1	1.4
Lithic fragment	< 20	–	–	–	–	–	2.0	12.7

TABLE 2. Relative Abundances of Helium, Neon, and Argon Isotopes from Individual Spherules and Fines of 15426, 43

Sample	^{4}He (10^{10} atoms/10^{-4} g)	$^{4}He/^{3}He$ (±10%)	$^{4}He/^{20}Ne$ (±10%)	$^{4}He/^{36}Ar$ (±10%)	$^{20}Ne/^{22}Ne$ (±5%)	$^{21}Ne/^{22}Ne$ (±5%)	$^{36}Ar/^{38}Ar$ (±5%)	$^{40}Ar/^{36}Ar$ (±5%)
Green spherules								
1	340		27	340	11.5	0.10	4.2	5.7
2	250	800	17	206	12.8	0.07	4.9	9.5
3	300	500	16	296	12.1	0.08	4.1	15
Black spherules								
1	14		9	76	6.4	0.60	1.9	<1
1′	47		23	167	6.6	0.76	1.9	
2	28		18	175	9.3	0.70		
Devitrified spherules								
1	172		51	490	10.0	0.43	1.7	5.5
2	180		51	430	9.7	0.35	3.2	16
Fines (< 100 mesh)								
1	610		11	246	12.5	0.038	5.3	6.5
2	970		9	170	13.2	0.124		9.5

TABLE 3. Distribution of Helium, Neon, and Argon Isotopes in 15498, 37, 43, 54, 55

Sample	^4He (10^{10} atoms/10^{-4} g)	$^4He/^3He$ (±10%)	$^4He/^{20}Ne$ (±10%)	$^4He/^{36}Ar$ (±10%)	$^{20}Ne/^{22}Ne$ (±5%)	$^{21}Ne/^{22}Ne$ (±5%)	$^{36}Ar/^{38}Ar$ (±5%)	$^{40}Ar/^{36}Ar$ (±5%)
15498, 37								
Lithic fragment	430	62	8.1	41	11.7	0.16	3.6	3.5
Lithic fragment	63	30	6.4	26	11.8	0.16	3.1	5.1
Matrix	2370	1000	6.9	29	12.1	0.038	5.1	2.0
Matrix	1850	800	8.2	33	12.5	0.043	5.1	2.5
Matrix	276	–	4.7	23	12.5	0.040	5.1	2.0
Vein	1750	–	14	34	13.3	0.05	4.1	2.7
Vein	390	–	11	27	12.3	0.06	4.4	3.6
15498, 43								
Glass	2240	1850	23	28	11.7	0.068	5.2	1.9
Glass	1800	1900	21	29	11.5	0.061	5.1	2.0
Glass	5200	–	22	33	11.7	0.067	5.0	2.6
15498, 54								
Glass	1530	1850	27	85	12.4	0.033	4.9	7.6
Glass	2800	2300	30	53	13.0	0.053	5.3	1.4
15498, 55								
Glass	1560	1550	5.8	33	12.4	0.048	4.8	2.0
Glass	570	–	3.8	22	12.5	0.054	4.6	2.2
Glass	1130	–	5.5	33	12.9	0.045	4.8	2.1
Matrix	94	–	22	104	7.5	0.57	1.4	2.0
Matrix	101	–	28	100	5.8	0.44	1.9	5

TABLE 4. Distribution of Helium, Neon, and Argon Isotopes in 15555, 101

Location	^{4}He (10^{10} atoms/10^{-4} g)	$^{4}He/^{3}He$	$^{4}He/^{20}Ne$	$^{4}He/^{36}Ar$	$^{20}Ne/^{22}Ne$	$^{21}Ne/^{22}Ne$	$^{36}Ar/^{38}Ar$	$^{40}Ar/^{36}Ar$
Pyroxene	2950	2600 ± 200	80 ± 8	870 ± 90	12.9 ± 0.4	0.054 ± 0.02	3.5 ± 0.3	3.6
Vug	440	2400 ± 200	630 ± 60	5700 ± 600	13.3 ± 0.4	0.056 ± 0.02	5.2 ± 0.2	7

LIST OF ILLUSTRATIONS

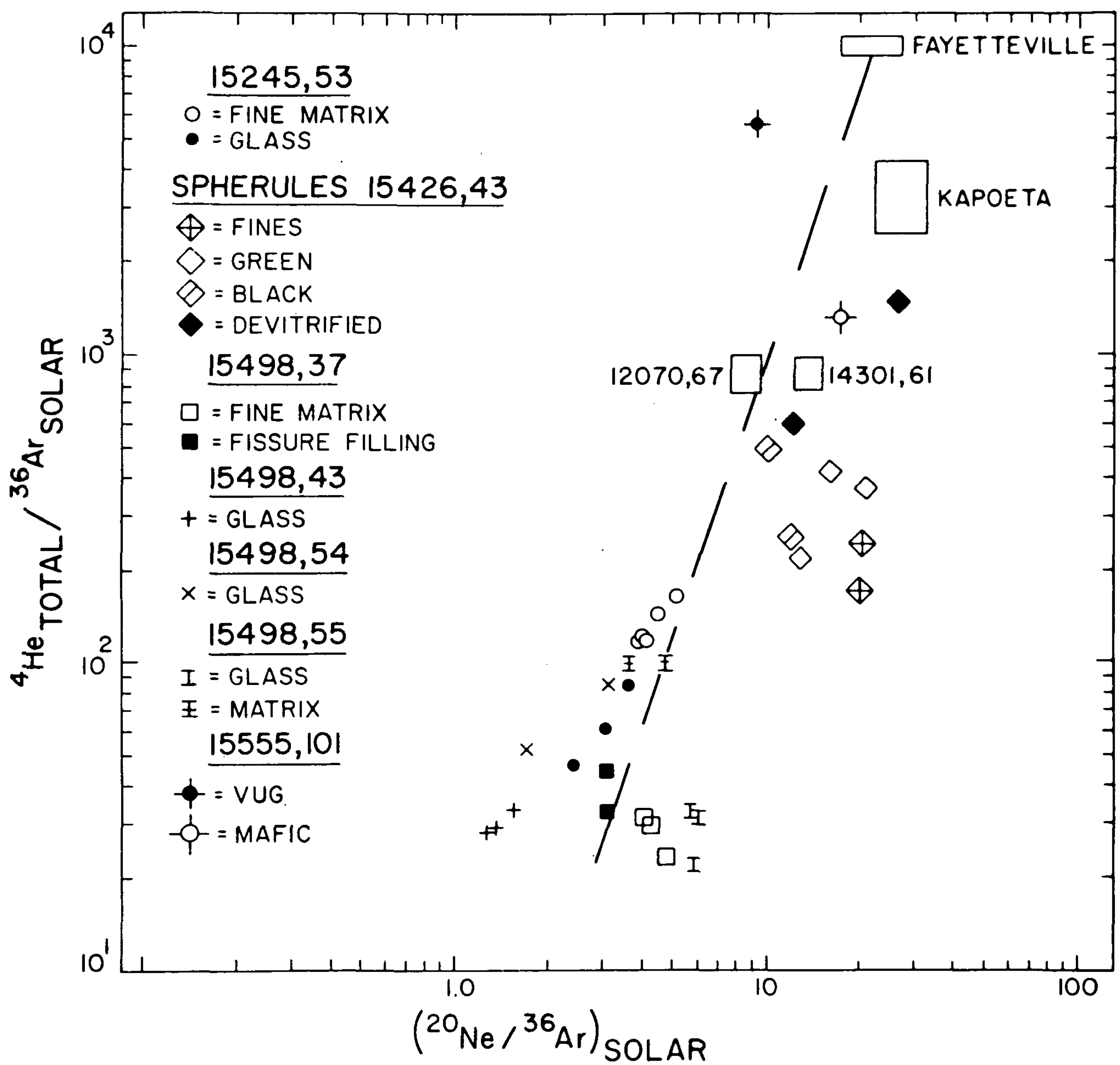
15245,53
○ = FINE MATRIX
● = GLASS
SPHERULES 15426,43
= FINES
= GREEN
= BLACK
= DEVITRIFIED
15498,37
□ = FINE MATRIX
■ = FISSURE FILLING
15498,43
+ = GLASS
15498,54
× = GLASS
15498,55
I = GLASS
= MATRIX
15555,101
= VUG
= MAFIC
FAYETTEVILLE
KAPOETA
12070,67
14301,61
$^{4}He_{TOTAL} / {}^{36}Ar_{SOLAR}$
$(^{20}Ne / {}^{36}Ar)_{SOLAR}$
10^{1}
10^{2}
10^{3}
10^{4}
1.0
10
100

Figure 1

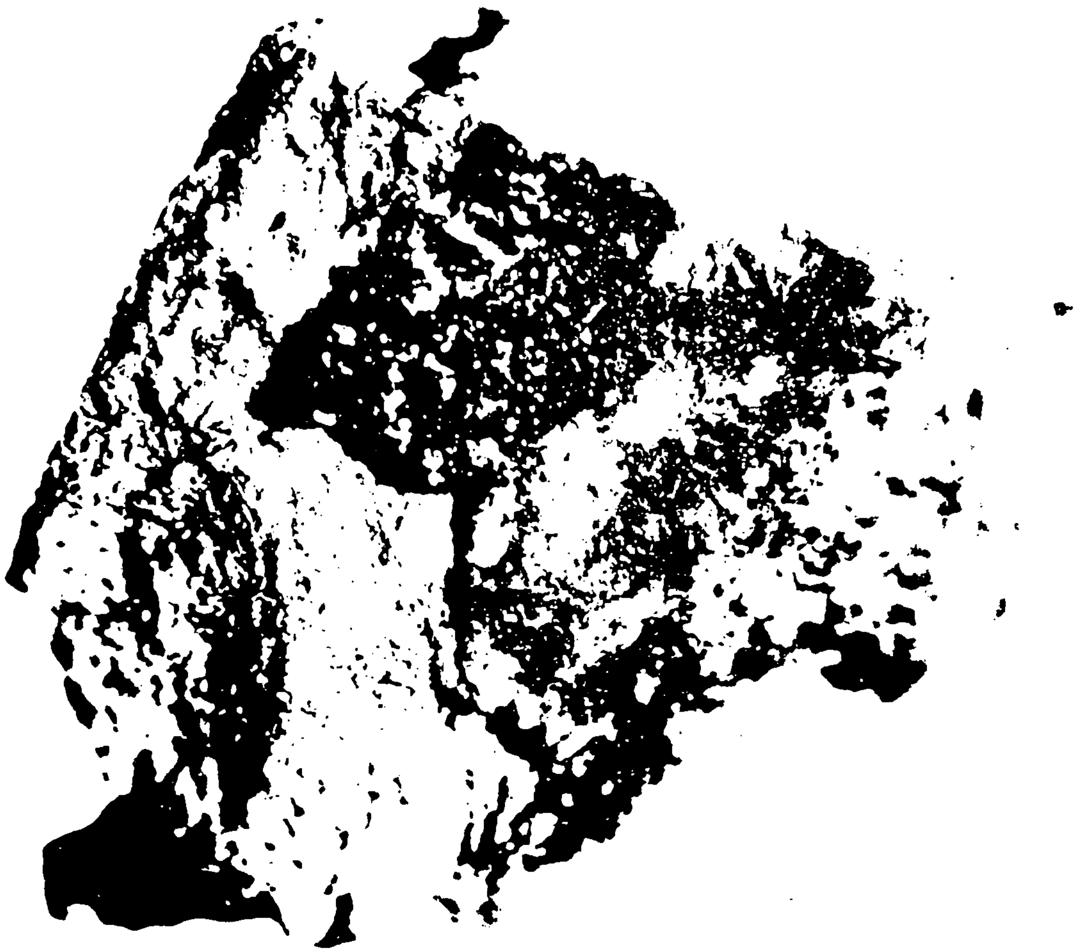

Figure 2

Figure 3

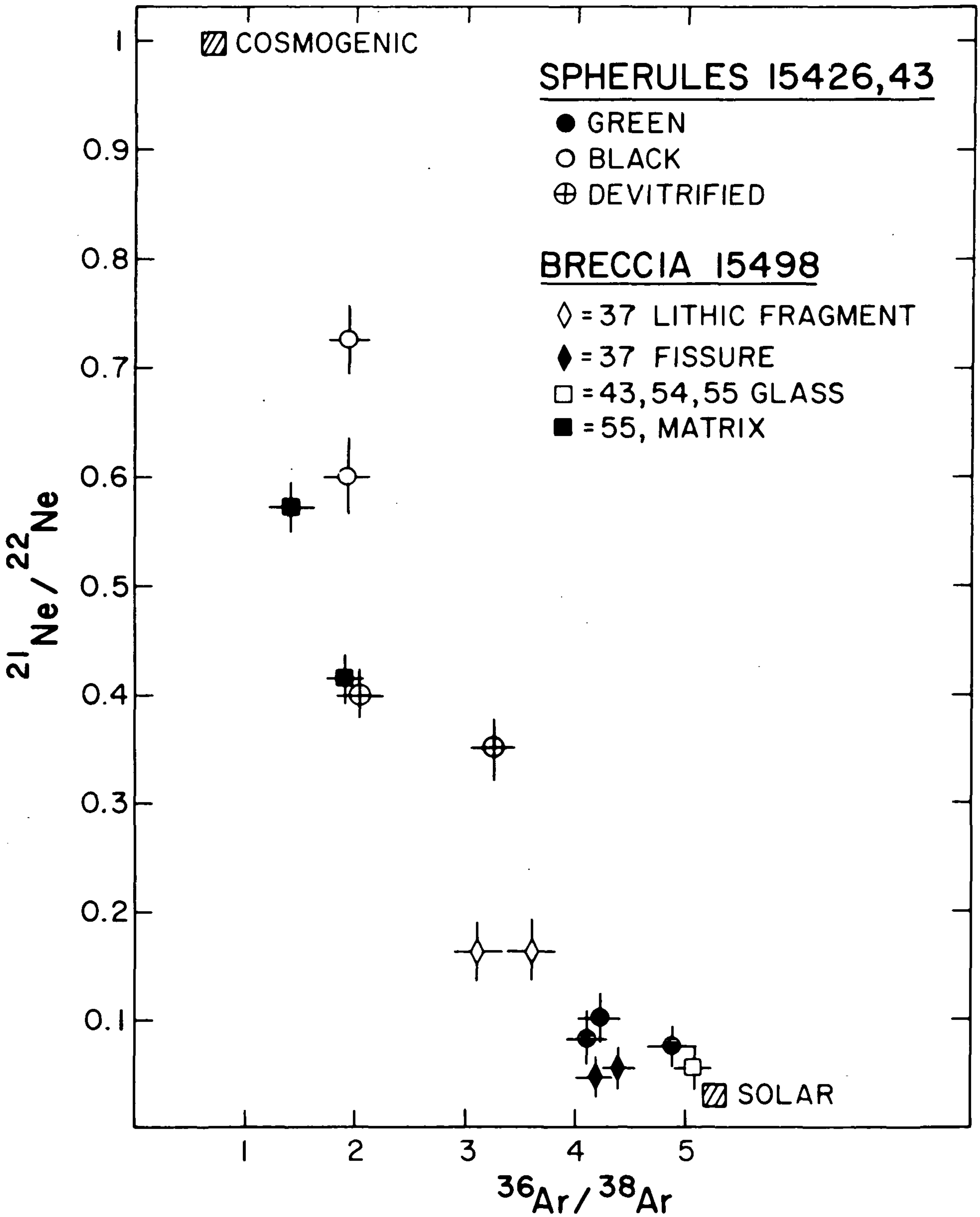
COSMOGENIC
SPHERULES 15426,43
GREEN
BLACK
DEVITRIFIED
BRECCIA 15498
= 37 LITHIC FRAGMENT
= 37 FISSURE
= 43,54,55 GLASS
= 55, MATRIX
SOLAR
$^{21}Ne/^{22}Ne$
$^{36}Ar/^{38}Ar$
1
0.9
0.8
0.7
0.6
0.5
0.4
0.3
0.2
0.1
1
2
3
4
5

Figure 4